Available online at www.sciencedirect.com
ScienceDirect
Ceramics International 35 (2009) 3021–3025
CERAMICS INTERNATIONAL
www.elsevier.com/locate/ceramint

Electrical and microwave dielectric properties of $K_2Nb_8O_{21}$ microwires

C.Y. Xu [a,b], L. Zhen [a,*], J.T. Jiang [a], C.S. Lao [b], L. Yang [a]

[a] School of Materials Science and Engineering, Harbin Institute of Technology, Harbin 150001, China
[b] School of Materials Science and Engineering, Georgia Institute of Technology, Atlanta, GA 30332, USA

Received 12 December 2008; received in revised form 3 March 2009; accepted 3 April 2009
Available online 24 April 2009

Abstract

$K_2Nb_8O_{21}$ microwires with diameters of several hundred nanometers and lengths up to tens of microns were prepared by molten salt synthesis, and characterized by X-ray diffraction, scanning electron microscopy and transmission electron microscopy. The as-synthesized microwires have semiconductor characteristics with band gap E_g of about 3.1 eV, consistent with electrical transport measurement of single microwire, which gives a resistivity of about 0.46 Ω m at room temperature. Microwave dielectric property measurement at 2–18 GHz shows that $K_2Nb_8O_{21}$ microwires have a relative low complex permittivity. A weak dielectric relaxation occurs in the 12–16 GHz band due to the free charges polarization on the interfaces between $K_2Nb_8O_{21}$ microwires and the PVB matrix.

Keywords: $K_2Nb_8O_{21}$ microwires; Molten salt synthesis (MSS); Electrical transport property; Microwave dielectric property

1. Introduction

One-dimensional (1D) nanostructures of ternary metal oxides might exhibit novel size-dependent properties, such as ferroelectric, multiferroic and nonlinear optical properties, which were the base for developing new nanodevices [1]. Various vapor and solution growth methods have been successfully utilized to fabricate ternary metal oxides 1D nanostructures, for example, alkali titanates [2], barium/strontium titanates [3], vanadates [4], niobates [5] and ABO_4-type chromates [6] and tungstates [7]. We have also developed a novel molten salt synthetic approach to fabricate a series of titanate and niobate 1D nanostructures, such as $Na_2Ti_6O_{13}$ and $KTi_8O_{16.5}$ nanowires [8], $K_2Ti_6O_{13}$ nanobelts [9], $K_2Nb_8O_{21}$ nanoribbons [10], and $NaNbO_3$ and $CaNb_2O_6$ nanorods [11].

Some recent work has shown that novel nanodevices could be designed using niobate 1D nanostructures based on their excellent nonlinear optical property. Yang and co-workers developed a subwavelength optical microscopy by employing tunable nanometric light source based on $KNbO_3$ nanowires [12]. Some other physical properties are expected to be explored in niobate 1D nanostructures for future applications. $K_2Nb_8O_{21}$ was found to be a stable phase in K_2O–Nb_2O_5 binary system [13], and its crystal structure belongs to the orthorhombic system with lattice parameters $a = 37.5$ Å, $b = 12.5$ Å and $c = 3.96$ Å [14]. The space group is $P2_12_12$ and the structure is that of the tungsten bronze type [15]. Recently, Teshima et al. reported that $K_2Nb_8O_{21}$ whiskers exhibited high photocatalytic activity for methylene blue absorption and degradation [16]. In this work, we prepared $K_2Nb_8O_{21}$ microwires via molten salt synthesis, and for the first time, measured the electrical transport property of single microwire. The microwave dielectric property of $K_2Nb_8O_{21}$ microwires/PVB composite in the range of 2–18 GHz was also investigated. These preliminary property investigations should be essential for developing single $K_2Nb_8O_{21}$ micro/nanowire-based nanodevices, such as gas sensor and UV-detector.

2. Experimental

$K_2Nb_8O_{21}$ microwires were synthesized by simply calcining Nb_2O_5 in excess KCl at 1000 °C. The chemical reaction for the synthesis of the $K_2Nb_8O_{21}$ microwires can be described as the

* Corresponding author. Tel.: +86 451 8641 2133; fax: +86 451 8641 3922.
E-mail address: lzhen@hit.edu.cn (L. Zhen).

0272-8842/$36.00
doi:10.1016/j.ceramint.2009.04.007

following formula:

$$8Nb_2O_5\,(s) + 4KCl\,(s) + O_2\,(g) \rightarrow 2K_2Nb_8O_{21}\,(s) + 2Cl_2\,(g) \quad (1)$$

In a typical procedure, 0.2 g Nb_2O_5 powders were mixed with 2.0 g KCl and ground for 10 min. The mixture was placed in a combustion boat and annealed in a tube furnace at 1000 °C for 3 h and, subsequently, cooled naturally to room temperature. The pristine powders were washed with distilled water several times, and then dried at room temperature.

The phase of the obtained microwires was examined by X-ray diffraction (XRD, Rigaku D/max-γB X-ray diffractormeter with Cu K_α radiation, $\lambda = 1.5406$ Å). The morphology and structure were characterized by scanning electron microscopy (SEM, LEO 1530) and transmission electron microscopy (TEM, Philips Tecnai 20). The microwires were dispersed in ethanol aided by ultrasonic treatment. One drop of the suspension was transferred to a holey carbon film supported on a copper grid for TEM observation.

UV–visible (vis) light diffuse reflectance spectrum of the synthesized microwires was obtained with a TU-1901 spectrometer. Electrical transport property of single microwire was measured at room temperature and ambient atmosphere. The as-synthesized microwires were dispersed in ethanol and then transferred onto a silicon substrate with pre-defined Au electrodes. In this way, the microwires were lying across the Au electrodes. In order to secure the contact between Au electrodes and microwire, Pt layer with thickness of about 500 nm was deposited using focused ion beam microscopy (FIB, Nova Nanolab 200).

Microwave dielectric property of the microwires was measured with a vector network analyzer (VNA, Agilent N5230A) in the frequency range of 2–18 GHz using Reflection/Transmission model. As for the specimen preparation, 20 vol.% $K_2Nb_8O_{21}$ microwires were randomly dispersed in polyvinyl butyral (PVB) and the mixture was pressed into a mould, in such a way toroidal specimens with outer diameter of 2.4 mm, inner diameter of 1.1 mm and thickness of about 3 mm were obtained. The reflection coefficient r and transmission coefficient t can be measured directly, and then the complex permittivity of the specimen is calculated through a computational algorithm described elsewhere [17].

3. Results and discussion

The morphology of the synthesized $K_2Nb_8O_{21}$ microwires was examined by SEM, as shown in Fig. 1a. Large quantity of microwires with diameters of several hundred nanometers was observed, indicating almost 100% yield of $K_2Nb_8O_{21}$ microwires. The length of $K_2Nb_8O_{21}$ microwires can reach up to several tens of microns, and most microwires tend to form bundles with diameters of several microns (Fig. 1b). Closer observations show that this 1D material has a faceted topography, as depicted in Fig. 1c. The faceted topography of the microwires might be due to the chemical interactions between the belts, and nanobelts could be obtained upon exfoliating under suitable experimental conditions [10].

The phase of the obtained microwires was examined by XRD, as shown in Fig. 2. The diffraction lines fit well with that of $K_2Nb_8O_{21}$ (JCPDS 31-1060) shown at the lower part, except

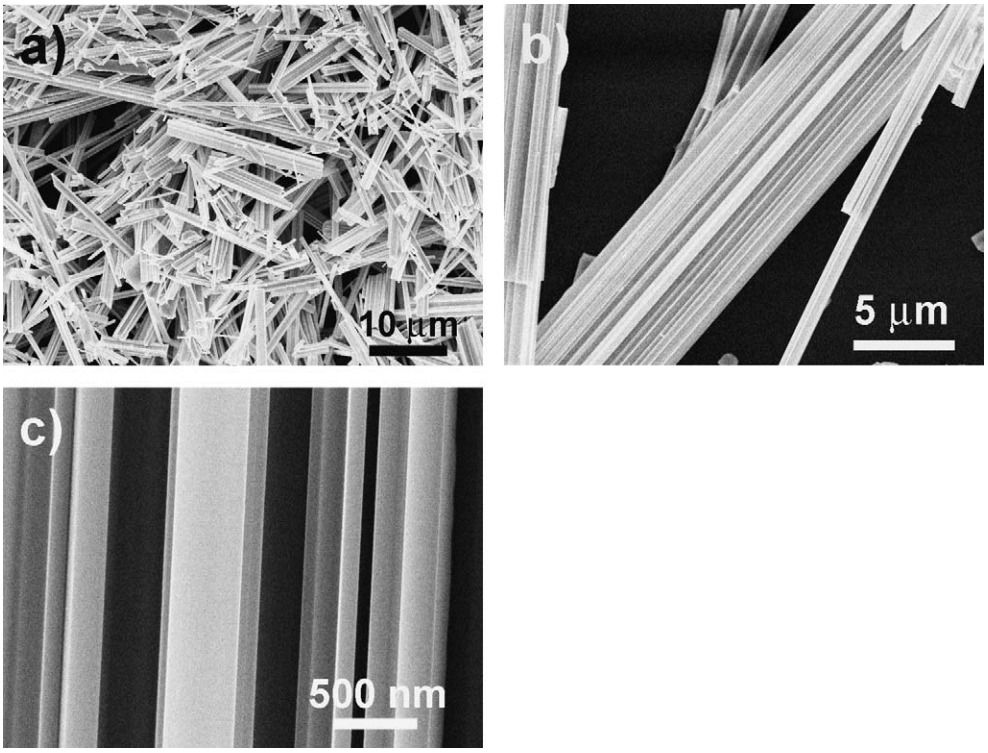

Fig. 1. (a) SEM image of $K_2Nb_8O_{21}$ microwires showing general morphology. (b) and (c) Large-magnification SEM images showing the bundle-like morphology of $K_2Nb_8O_{21}$ microwires with faced topography.

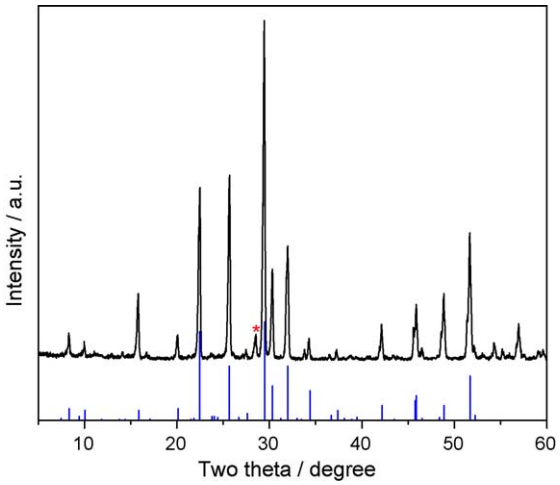

Fig. 2. XRD pattern of as-synthesized $K_2Nb_8O_{21}$ microwires. The angles for the standard sample of $K_2Nb_8O_{21}$ are shown at the lower part.

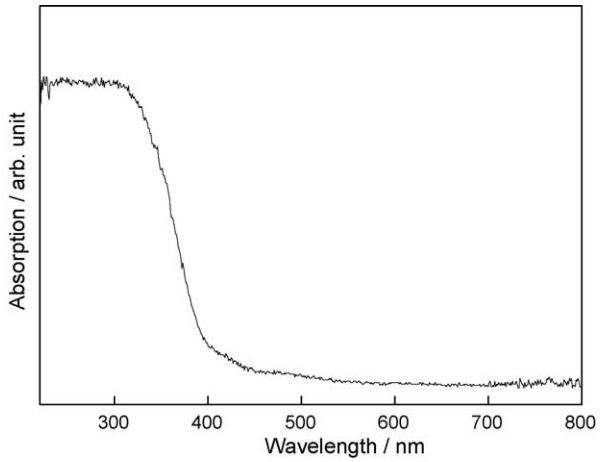

Fig. 4. UV–vis diffuse reflectance spectrum of $K_2Nb_8O_{21}$ microwires.

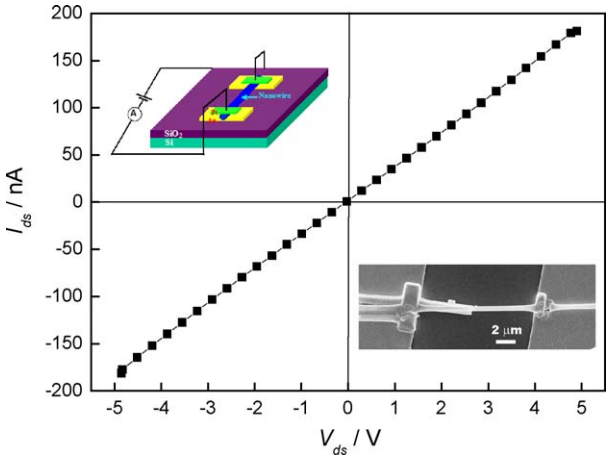

Fig. 5. *I–V* curve of single $K_2Nb_8O_{21}$ microwire with source-drain voltage $V_{ds} = 5$ V. The upper-left inset is the schematic showing the measurement system. The low-right inset is the SEM image of the measured microwire aligned between two Au electrodes.

that the diffraction line at 28.5° (marked with star) might be originated from KNb_3O_8 phase (JCPDS 39-0296). The crystal structure of $K_2Nb_8O_{21}$ belongs to the orthorhombic system with lattice parameters $a = 37.5$ Å, $b = 12.5$ Å and $c = 3.96$ Å [14].

Selected area electron diffraction (SAED) patterns taken from a wealth of microwires indicate that they are single-crystalline in nature. Fig. 3a shows TEM image of an individual microwire with diameter of about 300 nm, and its corresponding SAED pattern is shown in Fig. 3b. The diffraction pattern could be indexed to $[2\,\bar{3}\,0]$ zone axis of $K_2Nb_8O_{21}$, and the growth direction was determined to be its [0 0 1] crystallographic direction.

The UV–vis diffuse reflectance spectrum of $K_2Nb_8O_{21}$ microwire is shown in Fig. 4. The spectrum shows the onset wavelength of absorption at approximately 400 nm ($E_g = 3.10$ eV), indicating the semiconductor characteristics of the obtained microwires. Compared with that of the $K_2Nb_8O_{21}$ whiskers with average diameter of 8.3 μm [16], a blue shift of absorption edge was observed.

Electrical transport property of single microwire was measured at room temperature and ambient atmosphere. The schematic of experiment setup is illustrated in the up-left inset of Fig. 5. Fig. 5 shows the *I–V* characteristics of a single $K_2Nb_8O_{21}$ microwire, which was aligned between Au electrodes shown in the low-right inset. It shows good linear

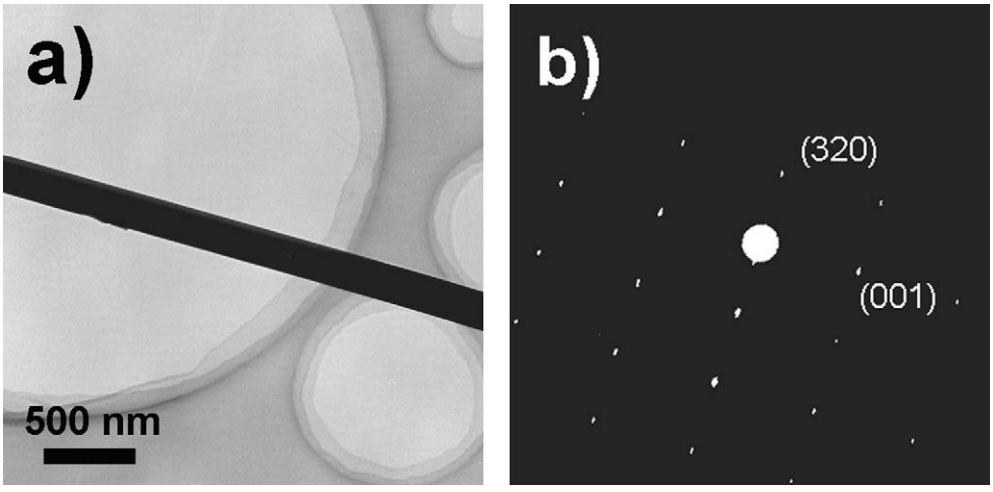

Fig. 3. (a) TEM image of an individual $K_2Nb_8O_{21}$ microwire, and (b) its corresponding SAED pattern.

relation between source-drain voltage and current, indicating the Ohmic contact between the measured microwire and Au electrodes. The electrical resistance of the selected microwire is $2.73 \times 10^7\ \Omega$. The electrical resistivity ρ of a material is usually defined by the following formula:

$$\rho = R\frac{A}{l} \tag{2}$$

where R is the electrical resistance of a uniform specimen, A the cross-sectional area, and l is the length of specimen.

As measured from the SEM image shown in the low-right inset of Fig. 5, the length of the measured microwire is about 12.3 μm, and the diameter is about 512 nm. Assuming that the microwires have circular cross-section, the electrical resistance of the measured $K_2Nb_8O_{21}$ microwire was calculated to be about 0.46 Ω m, showing the semiconductor characteristics of this material, which is consistence with that from UV–vis diffuse reflectance spectrum. The crystal structure of $K_2Nb_8O_{21}$ belongs to the orthorhombic system with space group of $P2_12_12$ and the structure is that of the tungsten bronze type [15]. Adjacent Nb–O octahedra are linked by sharing the vertices to form pentagonal, tetragonal and triangular channels running along the c direction, and the occupation of the pentagonal channels in the three subcells is different from one another, and it was assumed that two-third of the pentagonal channels are occupied by K atoms while the remaining ones are empty [15]. Based on the above structural investigation, it was postulated in the present work that the electrical conductance mechanism of $K_2Nb_8O_{21}$ is ionic conduction.

The complex permittivity of $K_2Nb_8O_{21}$ microwires/PVB composite is shown in Fig. 6. The real part of permittivity (ε') is about 5 and the imaginary part ε'' is fairly low. It should be noted that, a weak characteristic of dielectric relaxation, i.e., the decrease of ε' accompanied by the increase of ε'', is observed in the composite. A few VNA measurements with different sample thicknesses and measuring bands were carried out to confirm this phenomenon and the size or shape effects during the measurement were excluded, thus the observed relaxation behavior is ascribed to the intrinsic characteristics of $K_2Nb_8O_{21}$/PVB composite. This dielectric relaxation is believed to be originated from the free charges polarization in the $K_2Nb_8O_{21}$/PVB interface. It was found that free charges will gather in the conductor–insulator interfaces due to the disparity in electrical properties in a conductor–insulator composite. These free charges are polarized in an applied electromagnetic field and lead to the increase of permittivity in low frequency range. The free charges' polarization would be unable to follow the variation of the applied field when the frequency is higher than a certain value and a phase lag occurs, and thus a dielectric relaxation happens [18]. Similar behaviors have been observed in some composites such as metal/polymer and ceramics/polymer composites [19,20]. The dielectric relaxation usually falls into the optical or infrared band for composite containing high conductive metal particles [21,22], but the decrease in conductivity would lower the relaxation frequency $\upsilon_{rel.}$, even to microwave band [18]. The high electric

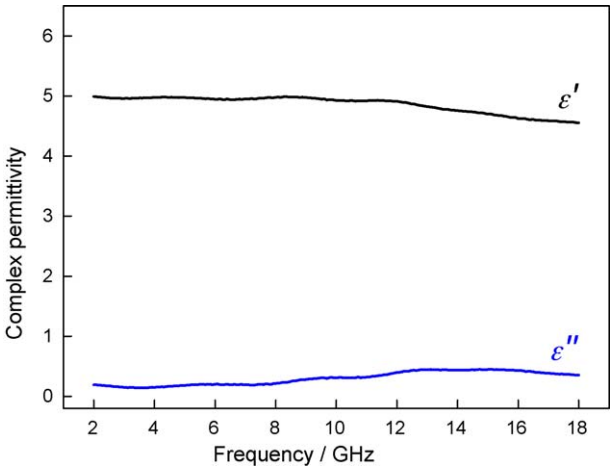

Fig. 6. Microwave dielectric property of $K_2Nb_8O_{21}$ microwires/PVB composite. Volume fraction of the microwires is 20%.

resistance of $K_2Nb_8O_{21}$ microwires may be the main reason for the low $\upsilon_{rel.}$ in the current study.

Additionally, the dielectric relaxation behavior observed in the current study is fairly weak compared with that observed in metal/polymer composites. This disparity might be due to the difference in conductance mechanism of the filler. As discussed above, the ionic conduction might be dominant for the $K_2Nb_8O_{21}$ microwires, which then leads to a low density of free charges in the interface since the conduction ions can hardly migrate to the $K_2Nb_8O_{21}$/PVB interface. Comparatively, in the case of metal fillers, the chargers are electrons that possess high migration ability and thus the density of the free charge in the interface is much higher.

4. Conclusions

In summary, $K_2Nb_8O_{21}$ microwires were synthesized on large scale by a facile molten salt approach. Electrical transport property of single $K_2Nb_8O_{21}$ microwire was measured, which shows the electrical resistivity is about 0.46 Ω m. A weak dielectric relaxation in 12–16 GHz band was observed in the $K_2Nb_8O_{21}$ microwires/PVB composite, which is due to the free charges polarization on the interfaces between $K_2Nb_8O_{21}$ microwires and the PVB matrix.

Acknowledgements

C.Y. Xu thanks Prof. Z.L. Wang for his kind permission to use facilities at Georgia Tech. This work was supported by the Development Program for Outstanding Young Teachers and Internationalization Foundation of HIT, and Postdoctoral Science Foundation of Heilongjiang Province (LBH-Z08112) and China Postdoctoral Science Foundation (No. 20080440126).

References

[1] Y.B. Mao, T.J. Park, S.S. Wong, Chem. Commun. (2005) 5761.
[2] X.M. Sun, X. Chen, Y.D. Li, Inorg. Chem. 41 (2002) 4996.

[3] J.J. Urban, W.S. Yun, Q. Gu, H.K. Park, J. Am. Chem. Soc. 124 (2002) 1186.
[4] J.G. Yu, J.C. Yu, W.K. Ho, L. Wu, X.C. Wang, J. Am. Chem. Soc. 126 (2004) 3422.
[5] A. Magrez, E. Vasco, J.W. Seo, C. Dieker, N. Setter, L. Forro, J. Phys. Chem. B 110 (2006) 58.
[6] J.H. Liang, C. Peng, X. Wang, X. Zheng, R.J. Wang, X.P. Qiu, C.W. Nan, Y.D. Li, Inorg. Chem. 44 (2005) 9405.
[7] H.T. Shi, L.M. Qi, J.M. Ma, H.M. Cheng, J. Am. Chem. Soc. 125 (2003) 3450.
[8] C.Y. Xu, Q. Zhang, H. Zhang, L. Zhen, J. Tang, L.-C. Qin, J. Am. Chem. Soc. 127 (2005) 11584.
[9] C.Y. Xu, Y.Z. Liu, L. Zhen, Z.L. Wang, J. Phys. Chem. C 112 (2008) 7547.
[10] C.Y. Xu, L. Zhen, L. Yang, K. He, W.Z. Shao, L.-C. Qin, Ceram. Int. 34 (2008) 435.
[11] C.Y. Xu, L. Zhen, R. Yang, Z.L. Wang, J. Am. Chem. Soc. 129 (2007) 15444.
[12] Y. Nakayama, P.J. Pauzauskie, A. Radenovic, R.M. Onorato, R.J. Saykally, J. Liphardt, P.D. Yang, Nature 447 (2007) 1098.
[13] X. Wu, L.S. Tang, Z.M. Fu, Y. Fang, W.X. Li, X.L. Huang, M.X. Zhao, Q.Z. Wu, J. Syn. Cryst. 13 (1984) 95 (in Chinese).
[14] C.M. Teng, F.H. Li, D.Y. Yang, Q.Z. Wu, J. Chin. Ceram. Soc. 4 (1986) 484 (in Chinese).
[15] F.H. Li, J. Microsc. 190 (1998) 249.
[16] K. Teshima, Y. Niina, K. Yubuta, T. Nakazawa, T. Suzuki, T. Shishido, N. Ishizawa, S. Oishi, Jpn. J. Appl. Phys. 47 (2008) 629.
[17] D.R. Smith, S. Schultz, Phys. Rev. B 65 (2002) 195104.
[18] N. Bowler, IEEE Trans. Dielect. Elect. Insul. 13 (2006) 703.
[19] I.J. Youngs, N. Bowler, K.P. Lymer, S. Hussian, J. Phys. D: Appl. Phys. 38 (2005) 188.
[20] D.L. Zhao, H.S. Zhao, W.C. Zhou, Phys. E 9 (2001) 679.
[21] R.D. Averitt, S.L. Westcott, N.J. Halas, Phys. Rev. B 58 (1998) R10203.
[22] S.J. Oldeberg, J.B. Jackson, S.L. Westcott, N.J. Halas, Appl. Phys. Lett. 75 (1999) 2897.